Long-Term Release Kinetics of Colloidal Particles from Natural Porous Media

ARTICLE *in* ENVIRONMENTAL SCIENCE AND TECHNOLOGY · OCTOBER 1999

Impact Factor: 5.33 · DOI: 10.1021/es990194m

2 AUTHORS:

Daniel Grolimund
Paul Scherrer Institut
155 PUBLICATIONS **3,549** CITATIONS
SEE PROFILE

Michal Borkovec
University of Geneva
234 PUBLICATIONS **12,846** CITATIONS
SEE PROFILE

Environ. Sci. Technol. **1999**, *33,* 4054−4060

Long-Term Release Kinetics of Colloidal Particles from Natural Porous Media

DANIEL GROLIMUND*

Department of Geological and Environmental Sciences, Stanford University, Stanford, California 94305-2115

MICHAL BORKOVEC

Department of Chemistry, Clarkson University, Potsdam, New York 13699-5814

Release of colloidal particles from natural porous media saturated with monovalent cations is studied with saturated laboratory column experiments packed with a noncalcareous soil material. The column outflow was monitored over 1000 pore volumes. The composition of released particles remains constant over the course of the experiment. The major finding of the present study is that the release process cannot be modeled with simple first-order kinetics, but the effluent concentration decays in a nonexponential fashion. The experimentally observed effluent concentration decays as $t^{-(1+\alpha)}$ where the exponent α typically has values between of 0.01 and 0.3. Such a power-law decay can be rationalized in terms of an exponential distribution of the activation energies of release rate coefficients, and the exponent α turns out to be inversely proportional to the average activation energy. We observe a strong dependence of the release on the ionic strength, which can be interpreted as a systematic increase of the average activation energy for particle release with increasing ionic strength. In the present system pH was accurately controlled, and the release pattern was surprisingly insensitive to pH variations.

Introduction

Mobile colloidal particles are omnipresent in the pore water of subsurface systems such as soils, groundwater aquifers, sediments, and fractured rocks (*1*−*4*). Several environmentally relevant phenomena are associated with the translocation of such submicrometer particles. Examples include structural damage of sodic soils, changes in hydraulic properties of aquifers due to artificial recharge, pore plugging during secondary oil recovery, or enhanced transport of strongly sorbing chemicals (*5*−*12*). Most frequently, mobile colloidal particles found in the subsurface are released from the surfaces of the porous matrix (*3, 4*), and the release process is commonly initiated by physical or chemical disturbances within the subsurface, such as changes in flow velocity or the chemical composition of the pore water.

Assessment of environmental quality issues within the subsurface requires the consideration of different remediation strategies and various wastewater management options. The decision making process leading to the optimal remediation strategy now heavily relies on quantitative computer models of water and solute transport in the subsurface. These approaches, in turn, call for model development of the pertinent physical, chemical, and biological processes. Enormous progress could be recently witnessed in the quantitative understanding of water flow and the various transport pathways of dissolved chemicals (*13*−*16*). However, as soon as mobilization and translocation of colloidal particles is involved in the transport pathway, our predictive capabilities are more limited (*4*). Assessing an environmental quality issue involving colloidal particles, we need a detailed understanding of the phenomena controlling particle deposition and release, and we must be able to rely on quantitative models, which are able to capture the main features of these processes.

Such understanding and model development can only evolve from experimental studies of particle release from natural porous media under well-controlled conditions. Only a limited number of investigations of this kind are available at present (*11, 17*−*20*). This paper presents probably the most extensive and complete data set on particle mobilization in natural porous materials available so far. The results originate from a series of long-term laboratory column experiments, where particle release was initiated by decreasing the ionic strength. While some authors have suggested that particle release can be modeled by first-order kinetics (*11, 12, 21, 22*), our results show unequivocally that the release kinetics is very different and can be only rationalized in terms of a very broad distribution of release rate coefficients.

In this publication we discuss results for a natural porous medium at constant pH and in the sole presence of monovalent cations, namely Na^+. In such a system, release of colloidal particles is easily achieved by decreasing the ionic strength. If, on the other hand, the system is fully saturated with divalent cations, such as Ca^{2+}, there is virtually no particle release. As will be discussed elsewhere, particle release is possible in systems saturated with a mixture of monovalent and divalent cations.

Experimental Section

Materials. As a model natural porous medium we used laboratory columns packed with noncalcareous soil aggregates. The soil material was collected from an (E)B horizon of a dystric Eutrochrept (Riedhof Soil), collected near Langenthal (Berne, Switzerland). The soil material is characterized by a silt loam texture (18% clay, 66% loam, 16% sand), as obtained by standard sieving and sedimentation analysis. Powder X-ray diffraction reveals a mineralogy dominated by vermiculite, illite, kaolinite, muscovite, and quartz, with traces of chlorite and goethite.

Additional measurements revealed an organic carbon content of 6 g kg^{-1}, pH of 4.1 measured in water, and a cation exchange capacity of ~70 μmol/g. Immediately after sample collection, the soil material was thoroughly mixed to generate a homogeneous batch, gently sieved to pass a 2-mm screen, air-dried, and stored at 4 °C in the dark. All solutions were prepared using water from a Barnstead Nanopure apparatus. The chemicals used were p.a. quality from Merck unless otherwise indicated.

Column Experiments. Soil aggregates ranging from 1.0 to 2.0 mm in diameter were separated by dry sieving and dry packed into glass chromatographic columns (Omnifit, Cambridge, U.K.) of 1 cm inner diameter and to a height of 36 ± 1 cm. The columns were preconditioned by a 0.5 M $CaCl_2$ solution for approximately 200 pore volumes. The solution was passed through a degasser (Erma) and pumped into the column by upward flow by a HPLC pump (Jasco) at a constant

* Corresponding author phone: +1 650 723 4782; fax: +1 650 725 2199; e-mail: daniel@pangea.stanford.edu.

10.1021/es990194m CCC: $18.00
Published on Web 10/08/1999

flow rate of 0.3 mL/min until full water-saturation was reached. The porous medium was then saturated by sodium by leaching the column with up to 1000 pore volumes of a 0.5 M NaCl solution, until the calcium concentration at the column outlet was below 10^{-7} M. Stabilization of the pH was achieved by leaching 300 pore volumes of a 0.5 M NaCl solution containing 15 mM sodium malonate buffer adjusted to pH 5.15. The presence of a buffering agent during the preequilibration as well as the entire experiment is required in order to control the pH conditions. This initial pH value was chosen to minimize the retardation of the second pH front in the release experiment. We also have added 1 mM sodium azide in order to avoid microbial activity. The described preequilibration procedure is essential to ensure identical initial conditions for each experiment. Column characteristics such as pore volume and dispersivities were determined in standard fashion by pulse experiments with NO_3^- as a conservative tracer (*15, 23, 24*). Characteristic column parameters were 19.4 ± 0.6 mL pore volume, porosities of 0.68 ± 0.02, and column Peclet numbers 60 ± 5 at a constant pore water velocity of $9.3 \cdot 10^{-5}$ m/s. These parameters were well reproducible with different column packings. These values lead to an average residence time t_0 of about 1.1 h and dispersivities of about 1.6 mm. At the column outlet, the pH was measured online with a flow-through combination electrode (Hamilton, microelectrode), and the effluent was subsequently collected by a fraction collector (Gilson).

Particle Release Experiments. Particle release was initiated by a step change from the preconditioning solution to an appropriate leaching solution of reduced ionic strength. Particle release was monitored up to 1000 pore volumes. In a first set of experiments, the effect of the electrolyte concentration on the particle mobilization was studied. The release was initiated by feeding the column with various solutions different in ionic strength adjusted to pH 5.25 with 15 mM sodium malonate buffer. In a second set of experiments, the effect of differences in pH on the release behavior of a natural porous medium was investigated. Particle mobilization was initiated by changing the ionic strength of the feed solution from 0.5 to 0.04 M. The experiment was carried out in the same way as the experiments at pH 5.25, but the final leaching solution was adjusted to pH 6.25. All column experiments were conducted at a room temperature of 24° ± 1 C.

Sample Analysis and Particle Characterization. The collected fractions were split into two samples to measure (i) the total concentrations of Na, Si, Al, and Fe, and (ii) the corresponding dissolved concentrations. Total elemental concentrations were obtained by inductively coupled plasma atomic emission spectroscopy (Varian Liberty 200 ICP-AES). Samples were acidified with distilled HNO_3 to pH < 2 and introduced into the plasma using an ultrasonic nebulization technique (Cetac U-5000AT). Suspended colloidal particles undergo complete atomization in the plasma as verified by comparison with acid digestion analysis. The dissolved concentrations of these elements were determined by ultracentrifugation of the sample (2 h at $2 \cdot 10^5$ g) and analyzing the supernatant in the same fashion. Particulate concentrations were calculated from the difference between total and dissolved concentrations. The dissolved concentrations of silica, aluminum, and iron were around $3 \cdot 10^{-6}$ M and were typically much smaller than the corresponding total concentrations. These elements were therefore used as indicators of suspended colloidal particles. The total and dissolved concentrations were equal within experimental error only for sodium. Particle concentrations were estimated by means of calibration curves obtained with dry samples of mobile colloidal particles (*10*). The detection limit of colloidal particles is related to the dissolved background concentration of the indicator elements. In the present study, this detection limit was approximately ~3 mg/L.

Experimental Results

General Features of Particle Release. Release of colloidal particles from a natural porous medium saturated with monovalent cations was investigated with a series of long-term leaching experiments of water-saturated laboratory columns packed with aggregates of a noncalcareous soil. In every experiment the column was extensively preconditioned with a solution of high ionic strength, where no significant particle release could be detected. This step is essential since traces of residual divalent cations (e.g., calcium) have a dramatic influence on particle release. Particle release was induced by leaching the column with a solution of lower ionic strength under controlled pH conditions.

Figure 1 summarizes a typical outcome of such an experiment. In this case, the column was preconditioned with 500 mM NaCl solution and is subsequently infiltrated with a solution of reduced total electrolyte concentration of 40 mM; for both solutions pH was appropriately controlled with 15 mM malonate buffer. The decrease in ionic strength results in release of colloidal particles from the porous matrix. No particles can initially be detected in the column effluent. As shown in Figure 1a, after one pore volume the particle concentration rises sharply to its maximum value, and thereafter the particle concentration decreases very gradually over several orders of magnitude in time, until the particle concentration falls below the detection limit. Particle release can be observed over nearly the entire experimental window of 1000 pore volumes which corresponds to an experimental duration of about 2 months. The linear appearance on the doubly logarithmic plot suggests a power-law type decay $t^{-(1+\alpha)}$ with the exponent α around 0.2.

The corresponding cumulative mass, as depicted in Figure 1b, rises very gradually even after 1000 pore volumes, and one might suspect that the total amount of released particles saturates around 20−30 mg/g.

The evolution of the solution composition is also shown in Figure 1. The sodium concentration in solution, as shown in Figure 1c, decreases sharply within a normality front at one pore volume and quickly approaches the concentration in the feed. The width of the front is mainly determined by dispersion phenomena. As evident in Figure 1d, the pH increases within the normality front due to the reduction in the ionic strength of the feed and quickly returns to the pH of the feed solution within a second retarded front (*25, 26*). Due to the presence of the buffer in the present system, the second front is hardly retarded, and equilibrium pH within the entire column is attained within 2−3 pore volumes. After this period, both chemical variables, namely the sodium concentration and the pH, remain constant during the whole experiment. Therefore, one can safely assume that the particle release process happens at constant chemical conditions. One should note, however, that without the presence of the buffer in the system, one typically needs 100−1000 pore volumes to attain the equilibrium with respect to the pH in the entire column.

The elemental composition of the released particles is virtually constant over the entire experiment. The absence of any trends in the elemental ratios of Si/Fe and Al/Si shown in Figure 1e suggests that the released particles do not undergo any fractionation during the release process. The elemental composition of the mobile particles is very similar to the clay fraction of the soil. For a very similar colloid release experiment in the absence of the buffer we have analyzed the mobilized particles by transmission electron microscopy and measured the particle size by dynamic light scattering (*10*). Both techniques have demonstrated that the particles size distribution is very broad, but the mass of the mobile

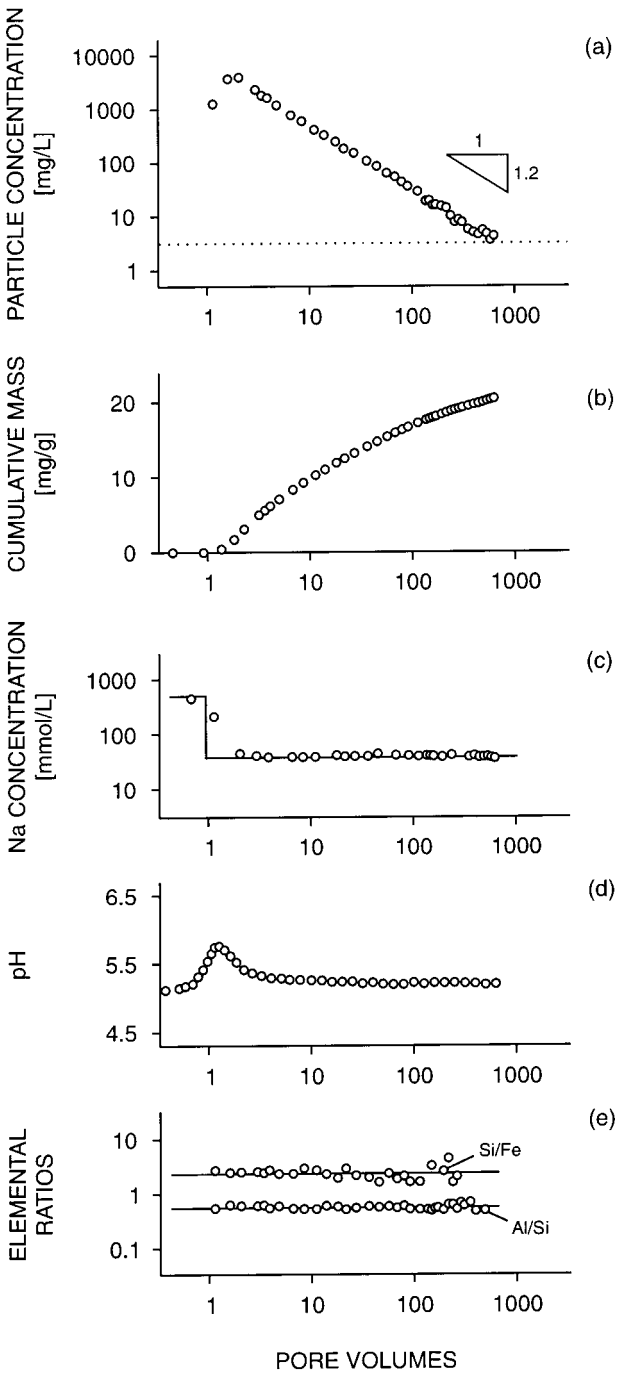

FIGURE 1. Typical mobilization experiment of colloidal particles from a natural porous material saturated with monovalent cations. The particle release is initiated by a stepwise change in ionic strength. (a) Particle concentration at the column outlet, the dotted line corresponds to the detection limit of 3 mg/L. (b) Cumulative mass, (c) sodium concentration, (d) pH at the column outlet, and (e) elemental ratios of Al, Si, and Fe of the suspended solids.

particles is dominated by particles in the range 0.1−0.5 μm in diameter.

Effect of Chemical Variables on Particle Release. The effect of the variation of the ionic strength is shown in Figure 2. Total ionic strengths of 20, 40, and 80 mM were investigated. Let us first focus on the experimental data points only. (The lines correspond to model calculations to be discussed later.) The particle concentration in the effluent is shown in Figure 2a, while the cumulative mass is shown in Figure 2b. With decreasing ionic strength the particle concentration in the effluent increases approximately by a constant factor through-

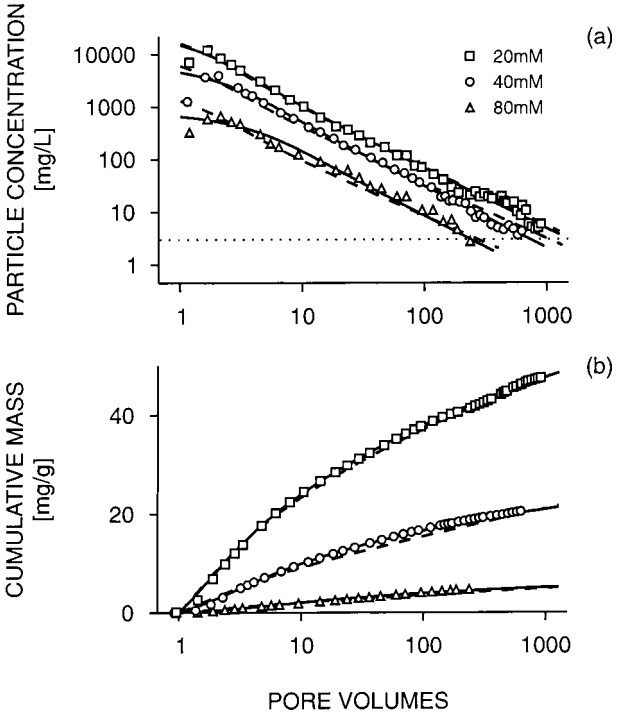

FIGURE 2. Dependence of the mobilization of colloidal particles from a natural porous material saturated with monovalent cations under controlled pH 5.25 (malonate buffer) on ionic strength: 20 mM (squares), 40 mM (circles), and 80 mM (triangles). (a) Particle concentration at the column outlet. The dotted line represents the detection limit. (b) Cumulative mass evolution. Effluent curves and cumulative mass are simultaneously fitted assuming an unconstrained exponential distribution of activation energies (solid lines) and by fixing the initial particle mass Q and the fast release rate constant k_0 (dashed lines). For optimized parameter values see Table 1.

out the entire experiment. However, the time dependence of the concentration profile remains similar for all ionic strengths leading to a power-law type decay $t^{-(1+\alpha)}$ with the exponent α around 0.17 ± 0.03.

Within the range of one pH unit, the particle release process is practically pH independent. The data shown in Figure 3 illustrate this aspect. The concentration profiles of released particles at pH 5.25 and 6.25 overlap almost entirely. This independence is probably related to the fact that the soil material is dominated by fixed charge clay minerals, which are only moderately dependent on pH. Unfortunately, the study of the pH effect over a wider pH range is nontrivial. Without the use of buffers, it is basically impossible to achieve constant pH conditions within the entire column in a reasonable time. To cover a wide pH range, one has to use different buffers, but each of these buffers will also influence the release in a specific way.

Modeling Particle Release

Single Particle Population. The transport of colloidal particles in a porous medium is characterized by the time evolution of the suspended particle concentration $c(x,t)$ per unit pore volume in water and the concentration of adsorbed particles $q(x,t)$ per unit dry mass. These two concentration profiles are both functions of the column depth x and time t. Our chromatographic column is dominated by convection, and we can thus neglect dispersion processes to a first approximation. In this case the two concentration profiles

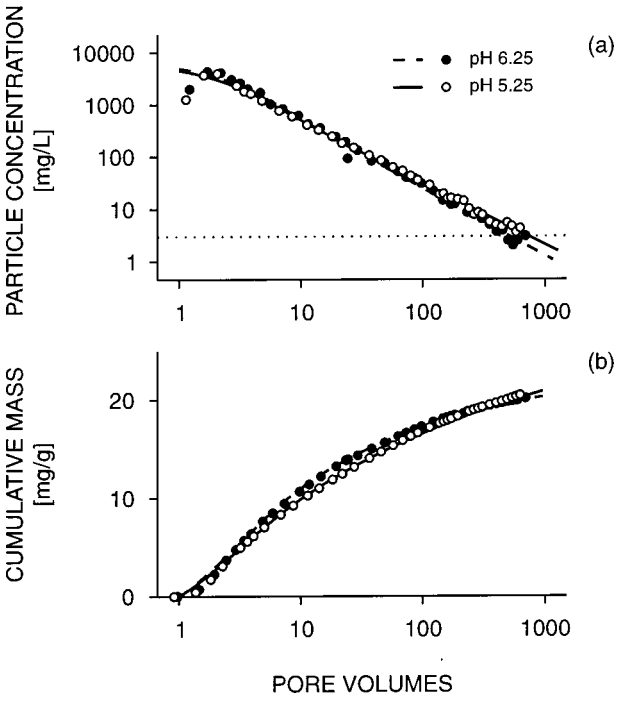

FIGURE 3. Dependence of the mobilization of colloidal particles from a natural porous material saturated with monovalent cations on pH. Open symbols correspond to pH 5.25 and solid symbols to pH 6.25. (a) Particle concentration at the column outlet. The dotted line represents the detection limit. (b) Cumulative mass evolution. Effluent curves and cumulative mass are simultaneously fitted assuming an unconstrained exponential distribution of activation energies (pH 5.25 solid lines, pH 6.25 dashed lines). For optimized parameter values see Table 1.

are linked by a simple convection equation

$$\frac{\partial c}{\partial t} + \frac{\partial q}{\partial t} = -v\frac{\partial c}{\partial x} \tag{1}$$

where v corresponds to the interstitial velocity of the particles. If we assume that there is no particle deposition and that the particle release process conforms to a first-order kinetic rate, then

$$\frac{\partial q}{\partial t} = -qk \tag{2}$$

where k is the release rate coefficient. In our situation, however, particle release is now induced by a normality front traveling with a velocity v. Equation 2 therefore applies only for $t \geq x/v$, while for $t < x/v$ we have $\partial q/\partial t = 0$.

For a semi-infinite porous medium in the absence of dispersion, there is only one relevant boundary condition, and it corresponds to vanishing particle concentration at column inlet. Initial conditions correspond to no suspended particles in solution, and a fixed uniform concentration of adsorbed particles Q per unit mass. With these boundary and initial conditions, the coupled set of equations (eqs 1 and 2) can be solved analytically, and the particle concentration in the column effluent can be shown to be

$$c(L,t) = \rho Q k t_0 e^{-k(t-t_0)} \tag{3}$$

where L corresponds to the column length, ρ to the solid mass per pore volume, and $t_0 = L/v$ is the mean residence time of a particle injected at the column inlet. Equation 3 applies only for $t \geq t_0$, while for $t < t_0$ the concentration of the effluent vanishes. A related experimental quantity is the cumulative mass of particles in the effluent which is given by

$$\tilde{Q}(t) = \frac{1}{\rho t_0}\int_0^t c(t,L)\, dt \tag{4}$$

and clearly we have $\tilde{Q}(t \to \infty) = Q$. Inserting eq 3 into eq 4 we find that the cumulative mass in the effluent is simply given by

$$\tilde{Q}(t) = Q[1 - e^{-k(t-t_0)}] \tag{5}$$

for $t \geq t_0$, while for $t < t_0$ we have $\tilde{Q}(t) = 0$. In principle, both quantities given by eqs 3 and 5 contain the same information, but in practice the experimental errors will enter rather differently. For this reason, proper data analysis requires the consideration of both quantities.

Single-exponential decay (cf. eqs 3 and 5) cannot explain the experimentally observed concentration profiles of mobile particles discussed earlier. A typical outcome of such an unsuccessful fitting attempt is shown in the left and middle columns of Figure 4. As evident from Figure 4a, the experimental particle concentration decays much more gradually than the model would predict, while the experimental cumulative mass rises much more slowly. We have used the initial amount of particles $Q = 19$ mg/g, and the release rate coefficient of $k = 0.09$ h^{-1}, but any other choice of parameters will only lead to a worse representation of the data. While this model fails so obviously when data over a wide range are available, a single exponential description can be successful with a limited window of experimental data. However, such a description is then only valid in the same window.

So far, several simplifications are inherent in our analysis, namely (i) neglect of dispersion processes, (ii) neglect of particle deposition, and (iii) assumption of equal travel velocities of colloidal particles and normality front. However, none of these simplifications can explain the poor performance of the single population model, as will be detailed now.

Neglect of Dispersion Processes. This simplification represents an excellent approximation, since we are dealing with columns with Peclet numbers around 60 and are mainly interested in elution curves up to 1000 pore volumes. Only within the first few pore volumes, where the particle concentration changes rapidly, dispersion can be important. By excluding the first few pore volumes of the elution curve in the analysis, any dispersion effects can be safely neglected.

Neglect of Particle Deposition. A simple criterion to ascertain the validity of this approximation is to show that the product of the deposition rate coefficient and the average residence time is not considerably larger than unity (*27*). For a very similar system as investigated here, the initial deposition rate coefficients have been measured in various background electrolytes (*28*). When the system is dominated by monovalent cations, the deposition rate coefficients are on the order of 1−2 h^{-1} in the concentration range of interest. Considering the typical residence times of 1.1 h, the relevant product is also in the order of unity and suggests that neglect of deposition is indeed justified. We have carried out detailed calculations to address the relevance of this effect and observe that deposition influences the results by less than 15%.

Assumption of Equal Travel Velocities for Colloidal Particles and the Normality Front. While colloidal particles travel faster than a conservative tracer due to size exclusion effects, the differences are rather small and typically on the order of 10−40% (*28*−*33*). We have analyzed the case of nonequal traveling velocities in detail by means of analytical solutions and numerical simulations. As a result of these calculations

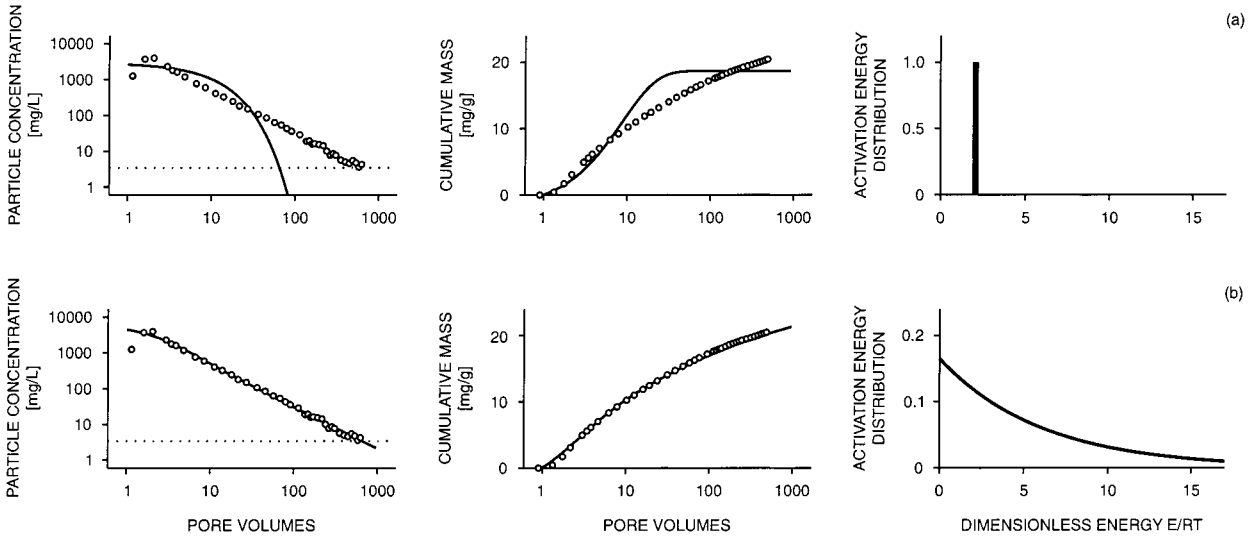

FIGURE 4. Fitting of the effluent data with different models. (a) Single population of particles and (b) exponential distribution of activation energies. The best fit is shown for the effluent concentration (left column) and the cumulative mass (middle column). The corresponding distributions of activation energies are also shown (right column).

it turns out that for our situation the expected differences to the case of equal velocities are minor indeed.

Multiple Particle Populations. The only remaining reason to explain the nonexponential elution curves of the released particles must be sought in the breakdown of eq 2. We shall incorporate this feature into the model by assuming multiple populations of colloidal particles, each of which decays exponentially analogue to eq 3 according to a particular rate coefficient. The existence of such a distribution should come as no surprise for a natural heterogeneous system, which is characterized by a wide particle size distribution, rough particle surfaces, heterogeneous mineralogical composition, and coatings on particle surfaces (*34*−*40*). However, similar nonexponential effects are also observed in simpler model systems, where such a heterogeneity in the adsorbed colloidal particle populations can be interpreted as originating from particles having different local environments due to imperfections of the surface, such as crevices, cracks, and the like (*41*−*44*).

Let us propose a plausible origin for the existence of a wide distribution of rate coefficients. This argument is standard in the discussion of relaxation of disordered systems (*45*) and turns out to be fully consistent with the present experimental data. The common understanding of particle detachment from surfaces is that the particle is trapped in an energy well and has to surmount an energy barrier in order to escape (*46*−*48*). The height of this energy barrier is just the activation energy E, and the release rate coefficient will depend on this activation energy through the Arrhenius law (*49*, *50*)

$$k = k_0 e^{-E/RT} \tag{6}$$

where RT is the thermal energy in molar units, and k_0 is the fast release rate coefficient, which reflects the rate in the absence of an activation barrier. The Arrhenius law originates from the fact that the rate coefficient is proportional to the probability of finding the escaping particle at the barrier top. This probability is precisely given by the exponential factor in eq 6.

The rate coefficient does sensitively depend on the activation energy, but its dependence on fast release rate coefficient is much weaker. Moreover, in the absence of barrier the particle release is primarily diffusion controlled, and therefore only a marginal dependence on the physicochemical parameters is expected (*20*). One can therefore make the rather reasonable assumption that the distribution of rate coefficients will solely originate from a distribution of activation energies. A reasonable choice for the distribution of the activation energies will be a thermal distribution, which is given by the exponential law

$$\rho(E) = \frac{1}{RT_0} e^{-E/RT_0} \tag{7}$$

This distribution reduces to the thermal distribution for $T_0 = T$, but as we shall see the interesting case actually occurs when the distribution is broader than the thermal distribution and the parameter T_0 is chosen such that $T_0 > T$. Since $E > 0$ the prefactor represents the appropriate normalization constant for this distribution. Clearly, eq 7 only represents a sophisticated guess for a distribution of activation energies, but, as we shall see, this guess is very reasonable indeed.

From eq 7 we can evaluate the distribution of rate coefficients, involving eq 6 and standard transformation of variables. The normalized distribution becomes

$$p(k) = \frac{\alpha k^{\alpha-1}}{k_0^{\alpha}} \tag{8}$$

for $0 < k < k_0$ and $p(k) = 0$ for $k_0 > k$. This relation is a simple power-law distribution, and the exponent is given by $\alpha = T/T_0$.

The last step in the analysis is to calculate the elution curves of colloidal particles from a porous medium, where the release rate constants are distributed according to a given probability distribution $p(k)$. Assuming that the different release events are statistically independent, one can simply average eq 3 over the probability density function. The result reads

$$c(L,t) = \rho Q t_0 \int_0^{\infty} p(k) k\, e^{-k(t-t_0)} dk \tag{9}$$

for $t \geq t_0$ and $c(L,t) = 0$ for $t < t_0$. We now insert the probability distribution eq 8 into eq 9 and obtain the explicit relation

$$c(L,t) = \rho Q \frac{\alpha k_0 t_0}{[k_0(t-t_0)]^{(\alpha+1)}} \gamma[1+\alpha, k_0(t-t_0)] \tag{10}$$

for $t \geq t_0$ and $c(L,t) = 0$ for $t < t_0$. We have introduced the

incomplete γ function (*51*)

$$\gamma[y,z] = \int_0^z x^{y-1}e^{-x}\,dx \qquad (11)$$

The corresponding result for the cumulative mass can be obtained by integration (cf. eq 5), and the result reads

$$\tilde{Q}(t) = Q\left[1 - \frac{\alpha}{[k_0(t-t_0)]^\alpha}\,\gamma[\alpha,k_0(t-t_0)]\right] \qquad (12)$$

for $t \geq t_0$, while for $t < t_0$ we have $\tilde{Q}(t) = 0$. This simple model therefore leads to analytical solutions for concentration profiles. The incomplete γ function is a standard special function available in most numerical libraries (e.g., (*52*)). From the properties of the incomplete γ function for $t \gg t_0$ we find that $c(L,t) \propto t^{-(\alpha+1)}$ and $Q - \tilde{Q}(t) \propto t^{-\alpha}$. This model indeed rationalizes the existence of power-law decay of the effluent concentration, and the exponent α now attains a precise physical meaning. This parameter is inversely proportional to the average activation energy for particle release. The previously estimated value of α around 0.2 means that the distribution of the activation energies is (about five times) wider than a thermal distribution—a fact which is again quite reasonable. A natural heterogeneous medium is far from equilibrium, and the distribution of energies will be naturally wider than in thermal equilibrium. The situation for $0 < \alpha < 1$ was analyzed in the literature rather thoroughly. The resulting power-law decay was reported for dispersive transport (*53*), dielectric relaxation (*54*), and, very recently, detachment of colloidal particles from glass surfaces (*55*). The resulting slow relaxation processes have been referred to as "fractal time" (*45*). Note that an entirely analogous argument can be put forward for the adsorption equilibrium and leads to the Freundlich isotherm (*56, 57*). The exponent α then becomes the Freundlich exponent.

The effluent concentrations obtained from the exponential distribution of activation energies (cf. eqs 10 and 12) are able to rationalize the experimental data quantitatively. Simultaneous least-squares fits of the effluent concentration and of the cumulative mass are shown in Figure 4b (left and middle column). These functions describe the data very well, and fitted parameters turn out to be $Q = 30.3$ mg/g, $k_0 = 0.71$ h^{-1}, and $\alpha = 0.17$.

The resulting distribution of activation energies is shown in Figure 4b (right column). For comparison we show the corresponding distribution of activation energies for the same value of k_0, and the actual exponential distribution of energies derived from the experiment. Naturally, a rather wide distribution of activation energies is needed.

We have analyzed the remaining experiments with the exponential distribution of activation energies in a similar fashion. The solid lines in Figures 2 and 3 are fits with the same exponential distribution when we adjust all parameters independently. An excellent fit of all the data is possible. Table 1 summarizes the resulting parameters, which are also represented graphically in Figure 5 (open symbols). The fast release rate coefficient k_0 decreases, and the exponent α increases with increasing ionic strength.

This unrestricted fitting procedure leads to the unphysical result that the total initial mass of the potentially mobile particles Q as well as the rate in the absence of a barrier k_0 depends on the ionic strength. We suspect that this is an artifact originating from too many fitting parameters. Clearly, one expects that the amount of mobile particles represents an inherent property of the system and should not vary with physicochemical conditions. Similarly, the rate in the absence of a barrier k_0 is primarily diffusion controlled, and one would expect to represent a constant as a first approximation. Therefore, we have repeated the same fitting procedure by

TABLE 1. Parameters of the Best Fits Using the Generalized Exponential Distribution

ionic strength [M]	pH	α [−]	k_0 [h^{-1}]	Q [mg/g]	rms[a] [−]
0.02	5.25	0.136	1.13	74.2	0.13
		0.098	1.36[b]	88.9[b]	0.14
0.04	5.25	0.165	0.71	30.3	0.08
		0.034	1.36[b]	88.9[b]	0.21
0.08	5.25	0.182	0.39	7.3	0.16
		0.007	1.36[b]	88.9[b]	0.21
0.04	6.25	0.281	0.64	22.9	0.17
		0.032	1.36[b]	88.9[b]	0.31

[a] Root-mean-square. [b] Kept constant during parameter optimization.

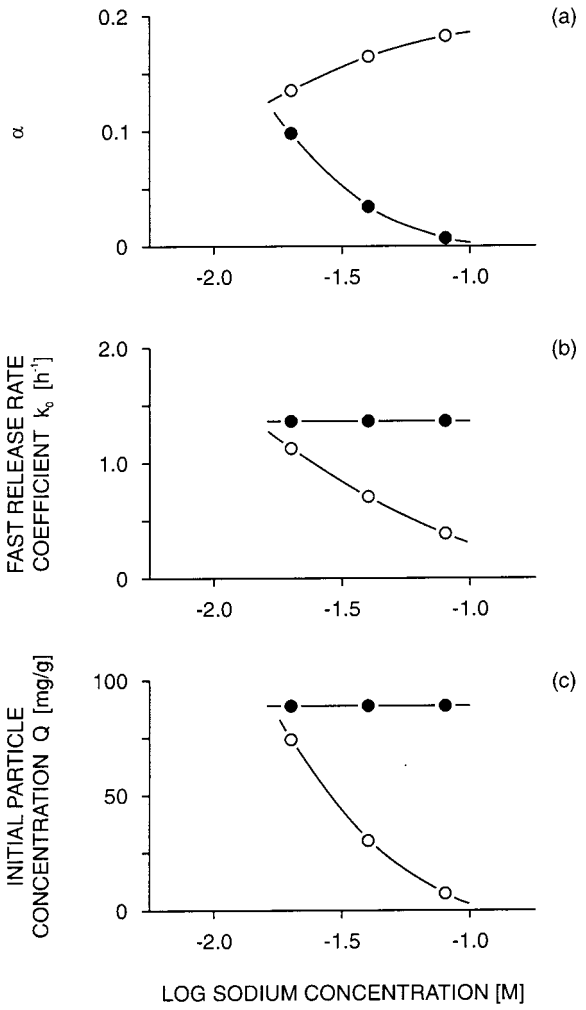

FIGURE 5. Effect of the ionic strength on the model parameters. (a) Exponent α, (b) fast release rate coefficient k_0, and (c) initial particle mass Q. Exponent α is inversely related to the average of the distribution of activation energies. Unconstrained fit (open symbols) is compared to a constrained fit using $Q = 89$ mg/g and $k_0 = 1.36$ h^{-1} (closed symbols).

fitting only the exponent α and fixing the other two parameters to the values $Q = 89$ mg/g and $k_0 = 1.36$ h^{-1}. The corresponding fits are shown as dashed lines in Figure 2 and confirm that this procedure yields almost equivalent results. The resulting parameter values are shown in Table 1 and are also summarized in Figure 5 (closed symbols). The resulting exponent α now decreases with increasing ionic strength. The value of the fixed total mass of $Q = 89$ mg/g, which is necessary to obtain a good fit for all experiments, corresponds to about 50% of the clay fraction. Since the largest particles

mobilized are about 0.5 μm in diameter, this analysis suggests that the entire fine clay fraction can be mobilized in such an experiment.

Assuming a constant total mass of colloidal particles Q and a constant fast release rate constant k_0, we conclude that the average activation energy increases with increasing ionic strength. For the boundary condition of constant surface charge, the height of the activation barrier for particle release has been shown to increase with increasing ionic strength (*47*), and one therefore expects the exponent a to decrease, in qualitative accord with the experimental results.

The observed power-law type decay of the released particles results in a considerable long-term susceptibility of natural porous media to repeated disturbances. Given the chemical variables fluctuate randomly, as expected from seasonal infiltration, large and long-term fluctuations in the particle concentration in the pore water will result. Due to the power-law decay discussed here, these fluctuations will have no inherent length scale and be of fractal character (*58*). The understanding of such fluctuations may be of substantial relevance in assessing the susceptibility of natural systems for phenomena induced by mobilized colloidal particles, such as enhanced transport of contaminants or structural damage of soils and aquifers.

Literature Cited

(1) McCarthy, J. F.; Degueldre, C. Sampling and characterization of colloids and particles in groundwater for studying their role in contaminant transport. In *Environmental Particles*; van Leeuwen, H. P., Buffle, J., Eds.; Lewis Publisher: Chelsea, MI, 1993.

(2) Degueldre, C.; Baeyens, B.; Goerlich, W.; Riga, J.; Verbist, J.; Stadelmann, P. *Geochim. Cosmochim. Acta* **1989**, *53*, 603−610.

(3) McCarthy, J. F.; Zachara, J. M. *Environ. Sci. Technol.* **1989**, *23*, 496−502.

(4) Ryan, J. N.; Elimelech, M. *Colloids Surfaces A* **1996**, *107*, 1−56.

(5) Jenny, H.; Smith, G. D. *Soil Sci.* **1935**, *39*, 377−389.

(6) Quirk, J. P. *Adv. Agronomy* **1994**, *53*, 121−183.

(7) Wiesner, M. R.; Grant, M. C.; Hutchins, S. R. *Environ. Sci. Technol.* **1996**, *30*, 3184−3191.

(8) Khilar, K. C.; Fogler, H. S. *Rev. Chem. Eng.* **1987**, *4*, 41−108.

(9) Fauré, M. H.; Sardin, M.; Vitorge, P. *J. Contam. Hydrol.* **1996**, *21*, 255−267.

(10) Grolimund, D.; Borkovec, M.; Barmettler, K.; Sticher, H. *Environ. Sci. Technol.* **1996**, *30*, 3118−3123.

(11) Roy, S. B.; Dzombak, D. A. *Colloids Surfaces A* **1996**, *107*, 245−262.

(12) Saiers, J. E.; Hornberger, G. M. *Water Resour. Res.* **1996**, *32*, 33−41.

(13) Dagan, G. *Flow and Transport in Porous Formations;* Springer: New York, 1989.

(14) Brusseau, M. L. *Rev. Geophysics* **1994**, *32*, 285−313.

(15) Sardin, M.; Schweich, D.; Leij, F. J.; van Genuchten, M. T. *Water Resour. Res.* **1991**, *27*, 2287−2307.

(16) Borkovec, M.; Bürgisser, C. S.; Cernik, M.; Glättli, U.; Sticher, H. *Trans. Por. Media* **1996**, *25*, 193−204.

(17) Khilar, K. C.; Fogler, H. S. *J. Colloid Interface Sci.* **1984**, *101*, 214−224.

(18) Goldenberg, L. C.; Magaritz, M.; Amiel, A. J.; Mandel, S. *J. Hydrol.* **1984**, *70*, 329−336.

(19) Seaman, J. C.; Bertsch, P. M.; Miller, W. P. *Environ. Sci. Technol.* **1995**, *29*, 1808−1815.

(20) Ryan, J. N.; Gschwend, P. M. *J. Colloid Interface Sci.* **1994**, *164*, 21−34.

(21) Lührmann, L.; Noseck, U.; Tix, C. *Water Resour. Res.* **1998**, *34*, 421−426.

(22) Corapcioglu, M. Y.; Jiang, S. *Water Resour. Res.* **1993**, *29*, 2215−2226.

(23) Villermaux, J. *Theory of linear Chromathography.* In *Percolation Processes: Theory and Applications*; Rodrigues, A. E., Tondeur, D., Eds.; Sijthoff & Noordhoff: Alphen aan den Rijn, The Netherlands, 1981; pp 83−140.

(24) Bürgisser, C. S.; Cernik, M.; Borkovec, M.; Sticher, H. *Environ. Sci. Technol.* **1993**, *27*, 943−948.

(25) Helfferich, F. G.; Klein, G. *Multicomponent Chromatography: Theory of Interference;* Marcel Dekker: New York, 1970.

(26) Scheidegger, A. M.; Bürgisser, C. S.; Borkovec, M.; Sticher, H.; Meeussen, J. C. L.; van Riemsdijk, W. *Water Resour. Res.* **1994**, *30*, 2937−2944.

(27) Jury, W. A.; Roth, K. *Transfer Functions and Solute Movement Trough Soils: Theory and Applications;* Birkhäuser: Basel, Switzerland, 1990.

(28) Grolimund, D.; Elimelech, M.; Borkovec, M.; Barmettler, K.; Kretzschmar, R.; Sticher, H. *Environ. Sci. Technol.* **1998**, *32*, 3562−3569.

(29) Higgo, J. J. W.; Williams, G. M.; Harrison, I.; Warwick, P.; Gardiner, M. P.; Longworth, G. *Colloids Surfaces A* **1993**, *73*, 179−200.

(30) Kretzschmar, R.; Robarge, W. P.; Amoozegar, A. *Water Resour. Res.* **1995**, *31*, 435−445.

(31) Kessler, J. H.; Hunt, J. R. *Water Resour. Res.* **1994**, *30*, 1195−1206.

(32) Vilks, P.; Frost, L. H.; Bachinski, D. B. *J. Contam. Hydrol.* **1997**, *26*, 203−214.

(33) Chrysikopoulos, C. V.; Abdel-Salam, A. *Colloids Surfaces A* **1997**, *121*, 189−202.

(34) Borkovec, M.; Wu, Q.; Degovics, G.; Laggner, P.; Sticher, H. *Colloids Surfaces A* **1993**, *73*, 65−76.

(35) Johnson, P. R.; Sun, N.; Elimelech, M. *Environ. Sci. Technol.* **1996**, *30*, 3284−3293.

(36) Coston, J. A.; Fuller, C. C.; Davis, J. A. *Geochim. Cosmochim. Acta* **1995**, *59*, 3535−3547.

(37) Ball, W. P.; Buehler, C.; Harmon, T. C.; Mackay, D. M.; Roberts, P. V. *J. Contam. Hydrol.* **1990**, *5*, 253−295.

(38) Jones, R. C.; Uehara, G. *Soil Sci. Soc. Am. Proc.* **1973**, *37*, 792−798.

(39) Hochella Jr., M. F.; Eggleston, C. M.; Elings, V. B.; Parks, G. A.; Brown Jr., G. E.; Wu, C. M.; Kjoller, K. *Am. Mineral.* **1989**, *74*, 1233−1246.

(40) Young, I. M.; Crawford, J. W. *J. Soil Sci.* **1991**, *42*, 187−192.

(41) Kallay, N.; Matijevic, E. *J. Colloid Interface Sci.* **1981**, *83*, 289−300.

(42) Kallay, N.; Biskup, B.; Tomic, M.; Matijevic, E. *J. Colloid Interface Sci.* **1986**, *114*, 357−362.

(43) Kallay, N.; Barouch, E.; Matijevic, E. *Adv. Colloid Interface Sci.* **1987**, *27*, 1−42.

(44) Kuo, R. J.; Matijevic, E. *J. Colloid Interface Sci.* **1980**, *78*, 407−421.

(45) Shlesinger, M. F. *Annu. Rev. Phys. Chem.* **1988**, *39*, 269−290.

(46) Dahneke, B. *J. Colloid Interface Sci.* **1975**, *50*, 89−107.

(47) Ruckenstein, E.; Prieve, D. C. *AICHE J.* **1976**, *22*, 276−283.

(48) Barouch, E.; Wright, T. H.; Matijevic, E. *J. Colloid Interface Sci.* **1987**, *118*, 473−481.

(49) Pauling, L. *General Chemistry;* W. H. Freeman & Co.: San Francisco, 1970.

(50) Stumm, W.; Morgan, J. J. *Aquatic Chemistry;* John Wiley: New York, 1996.

(51) Abramowitz, M.; Stegun, I. A. *Handbook of Mathematical Functions;* Dover: New York, 1970.

(52) Numerical Algorithms Group. *NAG Fortran Library*; Mark 16, Wilkinson House, Jordan Hill Road, Oxford, UK OX2 8DR.

(53) Scher, H.; Shlesinger, M. F.; Bendler, J. T. *Physics Today* **1991**, *44*, 26−34.

(54) Boettcher, C. J. F.; Bordewijk, P. *Theory of Electric Polarization;* Elsevier: Amsterdam, 1978; Vol. II.

(55) Weiss, M.; Lüthi, Y.; Ricka, J.; Jörg, T.; Bebie, H. *J. Colloid Interface Sci.* **1998**, *206*, 322−331.

(56) Sips, R. J. *J. Chem. Phys.* **1948**, *16*, 490−495.

(57) Sposito, G. *The Surface Chemistry of Soils;* Oxford University Press: New York, 1984.

(58) Feder, J. *Fractals;* Plenum Press: New York, 1988.

Received for review February 19, 1999. Revised manuscript received August 11, 1999. Accepted August 24, 1999.

ES990194M